Chiral recognition in the crystal structure of a dichiral mesogen with a unique isotropic mesophase: 2-{4-[(*R*)-2-fluorohexyloxy]phenyl}-5-{4-[(*S*)-2-fluoro-2-methyldecanoyloxy]phenyl}pyrimidine

Yasuko Matsunaga; Kayako Hori; Atsushi Yoshizawa; Tetsuo Kusumoto

PLEASE SCROLL DOWN FOR ARTICLE

Chiral recognition in the crystal structure of a dichiral mesogen with a unique isotropic mesophase: 2-{4-[(*R*)-2-fluorohexyloxy]-phenyl}-5-{4-[(*S*)-2-fluoro-2-methyldecanoyloxy]phenyl}pyrimidine

YASUKO MATSUNAGA, KAYAKO HORI*

Graduate School of Humanities and Sciences, Ochanomizu University, Otsuka, Bunkyo-ku, Tokyo 112-8610, Japan

ATSUSHI YOSHIZAWA

Faculty of Science and Technology, Hirosaki University, Hirosaki 036-8561, Japan

and TETSUO KUSUMOTO

Liquid Crystal Materials Division, Dainippon Ink & Chemicals, Inc., 4472-1 Komuro, Ina-machi, Kitaadachi-gun, Saitama 362-8577, Japan

The crystal structure of the title compound, which has an optically isotropic IsoX phase with an endothermic transition on cooling from an Sm*C phase, has been determined at 230 K. The crystal has a smectic-like layer structure composed of four crystallographically independent molecules. In the layer, one-dimensional chains of tightly fitted pyrimidine rings, with N … H distances shorter than the van der Waals radii, result in the large overlapping of core moieties and further induce close contacts and stereo-specific F–methyl interactions between the chiral groups; this is considered to be responsible for the uniquely organized IsoX phase.

1. Introduction

The compound 2-{4-[(*R*)-2-fluorohexyloxy]phenyl}-5-{4-[(*S*)-2-fluoro-2-methyldecanoyloxy]phenyl}pyrimidine, upon cooling, exhibits an endothermic transition from an Sm*C phase to an optically isotropic IsoX phase [1]. Recently the structure of the IsoX phase was found to be bicontinuous I*m*3*m* cubic by X-ray analysis [2]. Property–structure correlations for the compound indicate that the appearance of the IsoX phase is a chirality-dependent phenomenon [1, 3]. Slight modification of the compound, except for the terminal chain lengths, suppressed the IsoX phase [4]. Thus the IsoX phase is thought to be organized by a novel driving force for mesophase formation. In spite of much effort, a precise picture of the microscopic organization responsible for the novel transition phenomenon has not been obtained.

In order to obtain information on the packing mode of molecules of the compound and the driving force controlling the packing mode, its crystal structure has been determined.

2. Experimental

The compound was the same as previously studied [1–4]. Needle crystals were obtained by slow evaporation of an ethanol/ethyl acetate solution.

Cell parameters and reflection intensities were measured on an AFC-7R four-circle diffractometer using CuK$_\alpha$ radiation monochromated by graphite ($\lambda = 1.54184$ Å) at 230 K, because data obtained at room temperature gave only a poor result due to the high disorder of the terminal chains. The 2θ-ω mode was applied up to $2\theta = 136°$. Three standard reflections were measured after every 150 reflections; no significant variation was observed. The reflection data were corrected for Lorentz and polarization factors. In total, 12 737 reflections were collected, of which 9 003 were unique. R(int) = 0.090 for $I > \sigma(I)$. Crystal data for $C_{33}H_{42}O_3F_2N_2$: formula weight = 552.69, $T = 230$ K, triclinic, $P1$, $a = 10.161(3)$, $b = 32.725(13)$, $c = 10.021(3)$ Å, $\alpha = 94.43(2)°$, $\beta = 110.54(3)°$, $\gamma = 86.29(3)°$, $V = 3108.8(18)$ Å^3, $Z = 4$, $dx = 1.181$ Mg m^{-3}, $\mu = 0.675$ mm^{-1}.

The structure was solved by applying MULTAN88 [5] and refined by a four-blocked full-matrix least-squares method on F^2 by using SHELXL93 [6]. All the

*Author for correspondence; e-mail: khori@cc.ocha.ac.jp

Table 1.   Atomic coordinates and equivalent isotropic displacement parameters. U_{eq} is defined as one third of the trace of the orthogonalized U_{ij} tensor.

Atom	x	y	z	$U_{eq}/\text{Å}^2$
O(1A)	0.0240 (7)	0.5135 (2)	−0.3331 (7)	0.084 (2)
O(2A)	0.0495 (10)	0.4889 (2)	−0.5375 (8)	0.115 (3)
O(3A)	0.4238 (7)	0.8991 (2)	−0.5150 (7)	0.087 (2)
F(1A)	−0.1107 (8)	0.4277 (2)	−0.5609 (7)	0.037 (2)
F(2A)	0.6186 (9)	0.9861 (3)	−0.3287 (9)	0.067 (3)
C(1A)	0.3957 (10)	0.8608 (3)	−0.4857 (13)	0.069 (3)
C(2A)	0.3229 (10)	0.8364 (4)	−0.6049 (12)	0.076 (3)
C(3A)	0.2858 (9)	0.7978 (3)	−0.5926 (11)	0.067 (3)
C(4A)	0.3230 (9)	0.7826 (3)	−0.4555 (10)	0.066 (3)
C(5A)	0.3981 (11)	0.8070 (3)	−0.3408 (11)	0.073 (3)
C(6A)	0.4315 (11)	0.8457 (4)	−0.3567 (12)	0.090 (4)
C(7A)	0.2872 (10)	0.7416 (3)	−0.4389 (10)	0.062 (3)
N(1A)	0.1815 (9)	0.7249 (3)	−0.5475 (8)	0.045 (2)
C(9A)	0.1475 (10)	0.6891 (3)	−0.5244 (9)	0.070 (3)
C(10A)	0.2077 (9)	0.6669 (3)	−0.4010 (9)	0.063 (3)
C(11A)	0.3164 (10)	0.6893 (3)	−0.2978 (9)	0.079 (3)
N(2A)	0.3598 (9)	0.7257 (3)	−0.3130 (9)	0.054 (2)
C(13A)	0.1651 (10)	0.6281 (3)	−0.3784 (10)	0.064 (3)
C(14A)	0.0217 (10)	0.6184 (4)	−0.4294 (10)	0.078 (3)
C(15A)	−0.0229 (11)	0.5815 (4)	−0.4132 (11)	0.073 (3)
C(16A)	0.0716 (11)	0.5519 (4)	−0.3508 (11)	0.074 (3)
C(17A)	0.2157 (10)	0.5590 (3)	−0.2942 (10)	0.067 (3)
C(18A)	0.2636 (10)	0.5957 (3)	−0.3083 (9)	0.065 (3)
C(20A)	−0.1898 (10)	0.4598 (4)	−0.3827 (12)	0.098 (4)
C(21A)	0.0093 (10)	0.4863 (4)	−0.4383 (11)	0.080 (4)
C(22A)	−0.0642 (11)	0.4482 (4)	−0.4271 (12)	0.077 (3)
C(23A)	0.0406 (11)	0.4197 (4)	−0.3300 (12)	0.092 (4)
C(24A)	−0.0050 (11)	0.3790 (4)	−0.3172 (12)	0.093 (4)
C(25A)	0.1083 (12)	0.3541 (4)	−0.2092 (14)	0.115 (4)
C(26A)	0.0604 (15)	0.3147 (4)	−0.1794 (16)	0.125 (5)
C(27A)	0.1846 (18)	0.2910 (5)	−0.0654 (19)	0.165 (7)
C(28A)	0.139 (2)	0.2505 (5)	−0.0354 (19)	0.181 (8)
C(29A)	0.262 (2)	0.2280 (5)	−0.072 (2)	0.218 (10)
C(30A)	0.228 (2)	0.1867 (5)	0.103 (2)	0.260 (12)
C(31A)	0.5011 (12)	0.9245 (3)	−0.3941 (12)	0.096 (4)
C(32A)	0.5294 (12)	0.9644 (4)	−0.4504 (12)	0.106 (4)
C(33A)	0.3973 (15)	0.9914 (4)	−0.5122 (14)	0.118 (4)
C(34A)	0.4368 (15)	1.0321 (4)	−0.5453 (16)	0.122 (5)
C(35A)	0.3011 (19)	1.0602 (5)	−0.6129 (18)	0.166 (7)
C(36A)	0.327 (2)	1.0992 (5)	−0.6595 (21)	0.240 (12)
O(1B)	0.0112 (7)	0.5030 (3)	0.1540 (8)	0.088 (2)
O(2B)	0.0801 (8)	0.4721 (2)	−0.0197 (8)	0.091 (2)
O(3B)	0.4130 (8)	0.8903 (2)	0.0054 (8)	0.098 (2)
F(1B)	−0.0753 (8)	0.4095 (2)	−0.0424 (7)	0.038 (2)
F(2B)	0.4778 (13)	0.9619 (3)	0.2083 (11)	0.084 (4)
C(1B)	0.3858 (12)	0.8513 (3)	0.0193 (11)	0.071 (3)
C(2B)	0.2477 (11)	0.8405 (4)	−0.0430 (12)	0.085 (3)
C(3B)	0.2120 (10)	0.8024 (3)	−0.0328 (10)	0.071 (3)
C(4B)	0.3076 (11)	0.7732 (3)	0.0490 (9)	0.072 (3)
C(5B)	0.4499 (10)	0.7854 (4)	0.1093 (11)	0.077 (3)
C(6B)	0.4895 (11)	0.8226 (4)	0.0949 (10)	0.073 (3)
C(7B)	0.2664 (11)	0.7340 (3)	0.0663 (11)	0.073 (3)
N(1B)	0.1391 (9)	0.7212 (3)	−0.0187 (9)	0.056 (2)
C(9B)	0.1020 (10)	0.6854 (4)	0.0028 (10)	0.081 (3)
C(10B)	0.1894 (9)	0.6583 (4)	0.1040 (10)	0.084 (3)
C(11B)	0.3157 (10)	0.6768 (3)	0.1892 (10)	0.091 (4)
N(2B)	0.3601 (9)	0.7130 (3)	0.1734 (9)	0.054 (2)
C(13B)	0.1488 (10)	0.6175 (3)	0.1216 (10)	0.066 (3)
C(14B)	0.0649 (10)	0.5954 (4)	0.0002 (11)	0.079 (3)

Table 1.   (*continued*).

Atom	x	y	z	$U_{eq}/Å^2$
C(15B)	0.0205 (9)	0.5578 (3)	0.0054 (9)	0.070 (3)
C(16B)	0.0578 (10)	0.5401 (4)	0.1352 (11)	0.078 (3)
C(17B)	0.1447 (10)	0.5621 (3)	0.2638 (11)	0.071 (3)
C(18B)	0.1874 (10)	0.5994 (4)	0.2509 (10)	0.074 (3)
C(20B)	−0.1864 (11)	0.4437 (4)	0.1060 (15)	0.121 (5)
C(21B)	0.0214 (11)	0.4705 (4)	0.0673 (11)	0.075 (3)
C(22B)	−0.0458 (11)	0.4334 (4)	0.0833 (14)	0.092 (4)
C(23B)	0.0518 (12)	0.4089 (4)	0.2027 (13)	0.098 (4)
C(24B)	0.0129 (13)	0.3684 (4)	0.2218 (15)	0.112 (4)
C(25B)	0.1184 (14)	0.3454 (4)	0.3292 (15)	0.106 (4)
C(26B)	0.0749 (14)	0.3040 (4)	0.3501 (14)	0.115 (4)
C(27B)	0.1921 (18)	0.2779 (5)	0.4636 (17)	0.152 (6)
C(28B)	0.148 (2)	0.2363 (5)	0.483 (2)	0.183 (8)
C(29B)	0.268 (2)	0.2147 (6)	0.600 (2)	0.230 (11)
C(30B)	0.221 (3)	0.1740 (5)	0.630 (2)	0.287 (14)
C(31B)	0.5487 (12)	0.9060 (4)	0.0863 (14)	0.116 (5)
C(32B)	0.5369 (18)	0.9525 (5)	0.1098 (19)	0.157 (7)
C(33B)	0.4649 (15)	0.9723 (5)	−0.0259 (15)	0.128 (5)
C(34B)	0.458 (2)	1.0202 (5)	−0.0014 (18)	0.167 (7)
C(35B)	0.370 (3)	1.0413 (7)	−0.125 (2)	0.245 (12)
C(36B)	0.358 (3)	1.0868 (6)	−0.108 (2)	0.305 (17)
O(1C)	0.9615 (9)	0.8872 (3)	−0.0079 (11)	0.128 (3)
O(2C)	0.7906 (14)	0.9272 (4)	−0.003 (3)	0.218 (12)
O(3C)	0.5460 (7)	0.5063 (3)	0.1946 (8)	0.098 (2)
F(1C)	1.0607 (11)	0.9448 (3)	−0.1126 (12)	0.078 (3)
F(2C)	0.3471 (8)	0.4618 (3)	0.2713 (8)	0.044 (2)
C(1C)	0.5742 (11)	0.5438 (4)	0.1672 (11)	0.076 (3)
C(2C)	0.7158 (11)	0.5557 (4)	0.2312 (10)	0.076 (3)
C(3C)	0.7540 (10)	0.5935 (3)	0.2145 (10)	0.071 (3)
C(4C)	0.6564 (9)	0.6226 (3)	0.1298 (10)	0.059 (3)
C(5C)	0.5219 (10)	0.6090 (3)	0.0635 (9)	0.066 (3)
C(6C)	0.4806 (11)	0.5722 (4)	0.0833 (11)	0.084 (3)
C(7C)	0.6947 (11)	0.6619 (4)	0.1050 (9)	0.076 (3)
N(1C)	0.8263 (8)	0.6748 (3)	0.1974 (9)	0.055 (2)
C(9C)	0.8550 (10)	0.7112 (3)	0.1677 (10)	0.086 (3)
C(10C)	0.7725 (9)	0.7366 (3)	0.0619 (9)	0.062 (3)
C(11C)	0.6448 (10)	0.7180 (4)	−0.0211 (9)	0.081 (4)
N(2C)	0.6065 (8)	0.6824 (3)	−0.0037 (9)	0.044 (2)
C(13C)	0.8139 (10)	0.7754 (3)	0.0456 (9)	0.067 (3)
C(14C)	0.9014 (12)	0.8005 (3)	0.1595 (12)	0.081 (3)
C(15C)	0.9432 (11)	0.8388 (4)	0.1442 (13)	0.097 (4)
C(16C)	0.9032 (11)	0.8516 (3)	0.0080 (13)	0.074 (3)
C(17C)	0.8183 (12)	0.8307 (4)	−0.1035 (13)	0.090 (3)
C(18C)	0.7746 (11)	0.7926 (4)	−0.0862 (12)	0.087 (3)
C(20C)	1.1182 (16)	0.9586 (5)	0.1203 (17)	0.162 (6)
C(21C)	0.8993 (15)	0.9235 (4)	−0.0134 (16)	0.122 (5)
C(22C)	0.9958 (14)	0.9583 (4)	−0.0092 (13)	0.108 (4)
C(23C)	0.8925 (15)	0.9937 (4)	−0.043 (2)	0.173 (8)
C(24C)	0.9683 (17)	1.0311 (6)	−0.0609 (17)	0.164 (6)
C(25C)	0.845 (2)	1.0639 (6)	−0.124 (2)	0.222 (11)
C(26C)	0.899 (3)	1.0997 (7)	−0.168 (3)	0.295 (17)
C(27C)	0.765 (3)	1.1300 (11)	−0.216 (4)	0.31 (2)
C(28C)	0.805 (4)	1.1592 (11)	−0.294 (4)	0.38 (3)
C(29C)	0.693 (3)	1.1941 (9)	−0.342 (4)	0.36 (2)
C(30C)	0.747 (4)	1.2268 (9)	−0.404 (4)	0.411
C(31C)	0.4185 (10)	0.4897 (4)	0.0966 (10)	0.082 (3)
C(32C)	0.3974 (12)	0.4503 (4)	0.1541 (16)	0.121 (5)
C(33C)	0.5177 (11)	0.4218 (4)	0.1948 (13)	0.090 (3)
C(34C)	0.4919 (15)	0.3824 (5)	0.2425 (18)	0.135 (5)
C(35C)	0.6072 (17)	0.3537 (5)	0.2956 (19)	0.156 (6)

Table 1. (*continued*).

Atom	x	y	z	$U_{\mathrm{eq}}/\text{Å}^2$
C(36C)	0.5855 (18)	0.3142 (6)	0.349 (2)	0.203 (8)
O(1D)	0.9194 (8)	0.8708 (3)	0.4793 (9)	0.102 (3)
O(2D)	0.8360 (14)	0.9099 (4)	0.6255 (13)	0.103 (5)
O(3D)	0.5332 (7)	0.4921 (2)	0.7181 (8)	0.091 (2)
F(1D)	0.9473 (15)	0.9305 (3)	0.3515 (13)	0.111 (5)
F(2D)	0.3625 (10)	0.4407 (3)	0.7786 (10)	0.071 (3)
C(1D)	0.5621 (11)	0.5281 (4)	0.6869 (11)	0.079 (3)
C(2D)	0.6439 (10)	0.5535 (3)	0.8025 (10)	0.072 (3)
C(3D)	0.6759 (10)	0.5912 (4)	0.7772 (9)	0.072 (3)
C(4D)	0.6311 (10)	0.6061 (4)	0.6416 (10)	0.071 (3)
C(5D)	0.5548 (10)	0.5803 (4)	0.5272 (10)	0.076 (3)
C(6D)	0.5218 (9)	0.5424 (3)	0.5500 (12)	0.072 (3)
C(7D)	0.6697 (10)	0.6469 (4)	0.6202 (10)	0.082 (3)
N(1D)	0.7755 (9)	0.6643 (3)	0.7270 (9)	0.056 (2)
C(9D)	0.8093 (10)	0.7007 (4)	0.7018 (11)	0.091 (4)
C(10D)	0.7473 (10)	0.7214 (4)	0.5755 (11)	0.069 (3)
C(11D)	0.6356 (12)	0.6986 (4)	0.4761 (11)	0.099 (4)
N(2D)	0.5975 (10)	0.6622 (3)	0.4951 (9)	0.065 (3)
C(13D)	0.7908 (10)	0.7587 (4)	0.5544 (9)	0.069 (3)
C(14D)	0.9339 (11)	0.7699 (4)	0.6013 (12)	0.082 (3)
C(15D)	0.9773 (12)	0.8066 (4)	0.5798 (11)	0.088 (4)
C(16D)	0.8766 (11)	0.8356 (4)	0.5076 (11)	0.076 (3)
C(17D)	0.7299 (11)	0.8262 (5)	0.4586 (11)	0.097 (4)
C(18D)	0.6960 (13)	0.7887 (4)	0.4865 (12)	0.087 (3)
C(20D)	1.1153 (14)	0.9406 (5)	0.587 (2)	0.257 (14)
C(21D)	0.8891 (17)	0.9080 (5)	0.5443 (16)	0.119 (5)
C(22D)	0.9616 (16)	0.9399 (4)	0.4962 (14)	0.120 (5)
C(23D)	0.8808 (14)	0.9781 (4)	0.4977 (16)	0.128 (5)
C(24D)	0.9399 (16)	1.0151 (4)	0.4499 (17)	0.128 (5)
C(25D)	0.8240 (18)	1.0472 (5)	0.3984 (19)	0.167 (7)
C(26D)	0.8735 (18)	1.0854 (5)	0.353 (2)	0.172 (7)
C(27D)	0.757 (2)	1.1156 (6)	0.291 (3)	0.246 (13)
C(28D)	0.809 (2)	1.1525 (7)	0.247 (3)	0.249 (12)
C(29D)	0.694 (3)	1.1846 (7)	0.176 (3)	0.341 (17)
C(30D)	0.754 (3)	1.2215 (8)	0.144 (3)	0.361
C(31D)	0.4352 (11)	0.4675 (4)	0.6058 (11)	0.099 (4)
C(32D)	0.4129 (13)	0.4308 (4)	0.6694 (13)	0.154 (7)
C(33D)	0.5447 (12)	0.4028 (4)	0.7252 (13)	0.098 (4)
C(34D)	0.5179 (18)	0.3635 (5)	0.7734 (17)	0.150 (6)
C(35D)	0.643 (2)	0.3349 (5)	0.819 (2)	0.207 (10)
C(36D)	0.612 (2)	0.2957 (6)	0.879 (2)	0.236 (11)

non-hydrogen atoms were refined anisotropically. The displacement parameters of atoms in terminal chains, especially the 2-fluorohexyloxy group, were still large at 230 K; some were fixed. Hydrogen atoms, calculated geometrically (C–H distance: 0.97 Å for primary, 0.99 Å for secondary, and 0.94 Å for aromatic at 230 K), were included in structure-factor calculations but not refined. The atomic scattering factors were taken from *International Tables for Crystallography* [7]. Final results of refinements: $R1 = 0.1121$ and $Rw2 = 0.2726$ for 6358 observed reflections ($I > 2\sigma(I)$), $S = 1.767$, $(\Delta/\sigma)_{\mathrm{max}} = 0.217$, $\Delta\rho = 0.437$, $-0.355\,\text{e}\,\text{Å}^{-3}$. The large R values were attributable to the large thermal motions of the chains. Final atomic coordinates are listed in table 1.

3. Results and discussion
3.1. *Molecular structures*

Figure 1 shows the molecular structures with the numbering scheme of atoms. There are four crystallographically independent molecules, A, B, C and D. All the bond lengths and angles are normal within experimental error. The dihedral angles between the rings and the torsion angles of the chains are summarized in table 2. All the chains, C(22) to C(30) and C(31) to C(36) have approximately all-*trans*-conformations, although the large displacement parameters of terminal atoms indicate some degrees of disorder in the chains. Aromatic rings are twisted with respect to each other. The twist angles between rings C(1)–C(6) and C(7)–N(2)
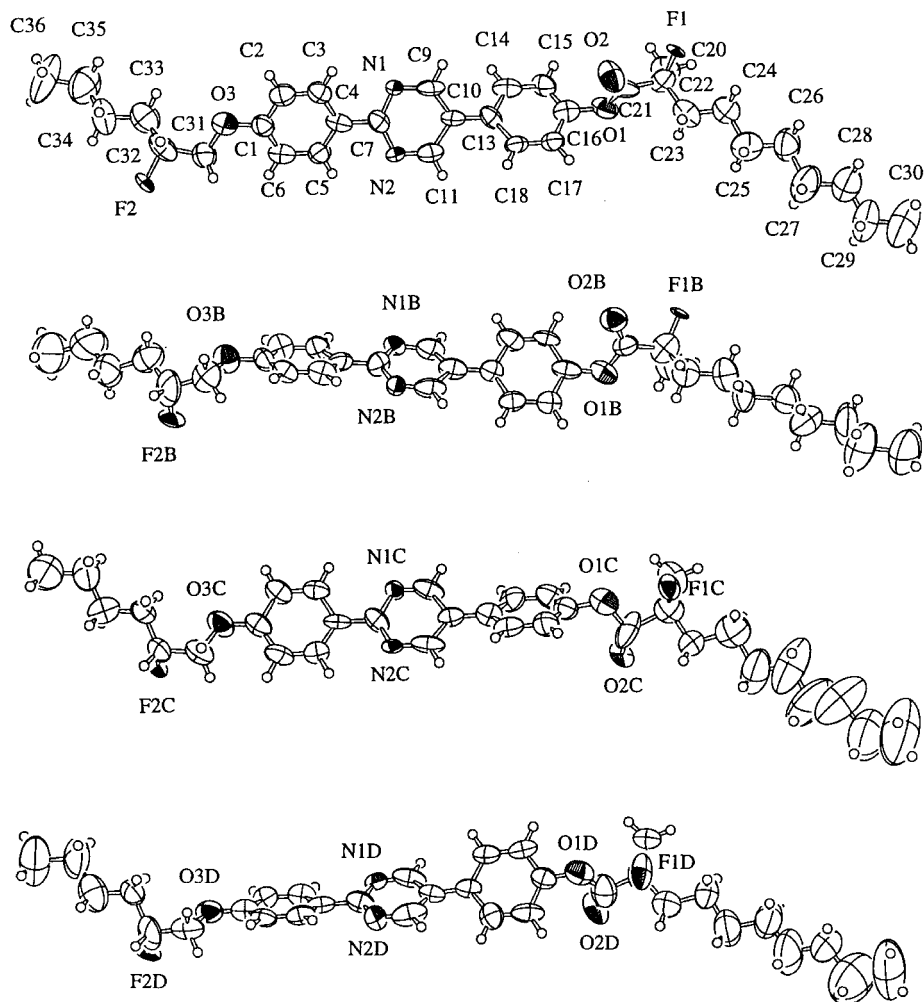
Figure 1. Molecular structures with 50% probability displacement ellipsoids. All the molecules are numbered with the same scheme.

Table 2. Dihedral angles of aromatic rings and torsion angles of chains.

	A	B	C	D
Ring (C1–C6)–ring(C7–N2)	18.4 (4)	16.0 (5)	14.5 (5)	17.1 (4)
Ring (C7–N2)–ring(C13–C18)	39.3 (3)	32.8 (4)	30.7 (4)	39.1 (4)
F1–C22–C23–C24	− 57.0 (13)	− 53.1 (14)	− 60.3 (18)	− 64.1 (16)
C20–C22–C23–C24	62.6 (14)	63.8 (15)	64 (2)	57.5 (19)
C21–C22–C23–C24	− 173.7 (9)	− 171.2 (11)	− 173.3 (13)	− 179.7 (12)
C22–C23–C24–C25	− 176.3 (9)	174.0 (11)	169.5 (15)	157.4 (14)
C23–C24–C25–C26	173.9 (11)	178.5 (11)	− 172 (2)	178.5 (14)
C24–C25–C26–C27	− 179.9 (11)	177.8 (13)	− 176 (2)	175.3 (19)
C25–C26–C27–C28	− 179.7 (13)	− 179.6 (14)	− 165 (3)	180 (2)
C26–C27–C28–C29	179.2 (17)	− 177.6 (17)	− 175 (3)	178 (2)
C27–C28–C29–C30	− 177.2 (19)	175.1 (18)	172 (4)	176 (3)
C1–O3–C31–C32	177.1 (8)	− 153.7 (12)	− 173.7 (10)	− 175.8 (10)
O3–C31–C32–F2	− 173.2 (8)	74.6 (17)	76.3 (11)	58.4 (14)
O3–C31–C32–C33	71.8 (12)	− 52.4 (18)	− 49.4 (16)	− 64.8 (12)
F2–C32–C33–C34	57.9 (13)	57.3 (18)	60.7 (15)	61.9 (16)
C31–C32–C33–C34	170.2 (10)	− 178.0 (14)	− 176.5 (12)	− 173.1 (11)
C32–C33–C34–C35	178.1 (11)	− 170.7 (19)	− 175.0 (16)	176.3 (16)
C33–C34–C35–C36	− 174.0 (14)	180 (2)	178.3 (15)	175.8 (14)

are smaller than those between rings C(7)–N(2) and C(13)–C(18), showing the steric effect of *o*-hydrogen atoms. Similar conformations were observed in 5-phenyl-2-(4-*n*-propoxyphenyl)pyrimidine (5-PPrPP) and 5-phenyl-2-(4-*n*-butoxyphenyl)pyrimidine (5-PBuPP), where the former rings are almost planar (5° and 8°, respectively) [8]. On the other hand, the three rings are almost coplanar (3–9°) in 2-phenyl-5-(4-*n*-pentoxyphenyl)-pyrimidine (2-PPePP) [9]. Similarly, the N-side benzene ring is less twisted (3°–12°) from the pyridine ring than from the opposite ring (28°–35°) for each of three crystallo-graphically independent molecules in (*S*)-2-(4-pentyl-phenyl)-5-[4-(1-methylheptyloxy)phenyl]pyridine, while the three rings are almost coplanar in (*S*)-2-[4-(1-methyl-heptyloxy)phenyl]-5-(4-pentylphenyl)pyridine [10].
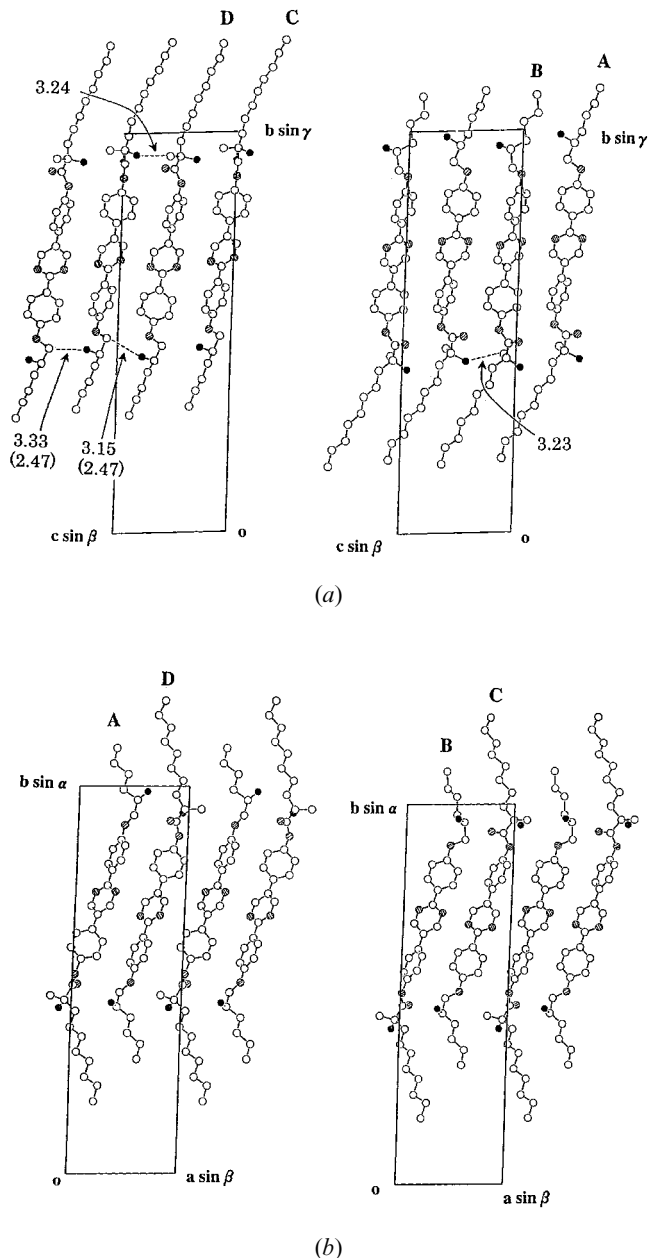

(*a*)

(*b*)

Figure 2. Crystal structure viewed along the *a* and *c* axes. Almost completely overlapped molecules are shown separately in each case. ●, ⊘, and ⊗ denote F, O, and N atoms, respectively. H atoms are omitted for simplicity. Numerical values are interatomic distances in Å for F atoms shorter than van der Waals contact distances. Those in parentheses are F … H distances.
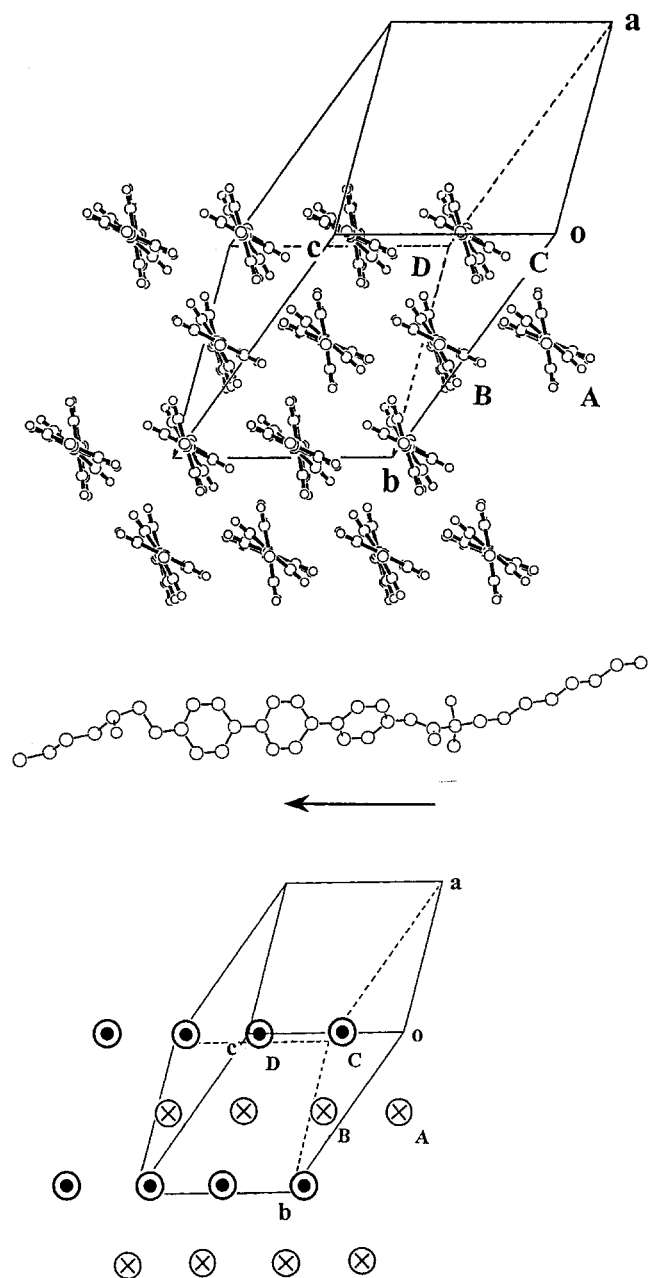

Figure 3. Crystal packing of core moieties viewed along the molecular long axes, where H atoms are included. The direction of the molecular long axis is also shown (lower).

3.2. *Crystal packing*

The crystal has a smectic-like layer structure with the layer plane parallel to the *ac* plane. The tilt angle of core moieties is estimated to be 20°. Figure 2 shows the crystal structure viewed along the *a* and *c* axes. Molecular pairs, A-B and C-D are separately shown in figure 2(*a*) because they almost completely overlap each other along the *a* axis. Similarly, molecular pairs A-D and C-B are separately shown in figure 2(*b*) because they almost completely overlap along the *c* axis. Molecular long axes are parallel along the *c* axis, while they are antiparallel along the *a* axis.

Figure 3 shows the molecular long axes packed in a pseudo-hexagonal array, as commonly observed in crystals of other calamitic mesogens [11, 12]. A characteristic feature, however, is observed in the arrangement of aromatic planes: they are almost parallel, in contrast to the usually observed herringbone arrangement of smaller aromatic rings [13]. Actually the herringbone arrangements are present in 2-PPePP and the two chiral diphenylpyridines mentioned above, while core moieties shift with respect to each other in 5-PPrPP and 5-PBuPP. Figure 4 shows the mutual arrangement of molecules, A-C and B-D, along the diagonal plane of the unit cell. Antiparallel pyrimidine rings fit closely with the N…H distances of 2.54–2.71 Å, shorter than the van der Waals radii (1.20 Å for H and 1.55 Å for N

[14]), indicating a strong interaction in addition to the dipolar interaction between the antiparallel pyrimidine moieties. Benzene rings are slightly twisted due to the repulsion of hydrogen atoms between neighbouring molecules. Table 3 shows that F(1A) and F(1C) atoms are closer (3.23 and 3.24 Å) than the van der Waals radii (1.47 Å for F and 2.0 Å for the methyl group [14]) to the chiral methyl C atoms, C(20B) and C(20D), respectively. In addition, F(2C) and F(2D) are very near to methylene H atoms of C(31D) and C(31C) adjacent to the chiral centre, respectively. These facts suggest strong interactions involving the chiral groups. It is also shown that F atoms are relatively close to the O atoms in the C=O bonds of ester linkages.

It is interpreted that the bulky chiral groups in both terminal chains prevent the molecules from packing in a regular herringbone arrangement. In such a situation, however, the molecules have some degrees of freedom, leading the pyrimidine rings to pack closely. Then, the strong interaction between the antiparallel pyrimidine rings leads to a large overlapping of core moieties and hence the chiral groups, as schematically shown in

Table 3. Interatomic distances involving F atoms and ester linkages. The van der Waals radii are 1.47, 1.52, and 1.70 Å for F, O, and C atoms, respectively, and 2.0 Å for the methyl group [14]. The symmetry code (x, y, z) is omitted.

| Atom	Pair	Distance/Å
F(2C)	C(31D)	3.15(1)
F(1B)	C(24A)	3.16(1)
F(2D)	C(23A) $(x, y, z + 1)$	3.17(1)
F(1A)	C(20B) $(x, y, z - 1)$	3.23(2)
F(2A)	C(23C)	3.23(2)
F(2C)	C(21B)	3.23(1)
F(1C)	C(20D) $(x, y, z - 1)$	3.24(2)
F(2B)	C(33A) $(x, y, z + 1)$	3.25(1)
F(1B)	C(25A)	3.29(1)
F(1A)	C(24B) $(x, y, z - 1)$	3.32(1)
F(2D)	C(31C) $(x, y, z + 1)$	3.33(1)
F(1A)	C(23B) $(x, y, z - 1)$	3.33(1)
F(2B)	C(34A) $(x, y, z + 1)$	3.36(1)
F(2C)	C(23B)	3.39(1)
F(1C)	O(2D) $(x, y, z - 1)$	3.01(1)
F(2C)	O(2B)	3.23(1)
O(2A)	O(1B) $(x, y, z - 1)$	3.05(1)
O(1A)	O(2B)	3.37(1)
O(2C)	C(31B)	3.03(1)
O(2B)	C(32C)	3.15(1)
O(2C)	C(32B)	3.20(2)
O(2B)	C(31C)	3.30(1)
O(1C)	C(2B) $(x + 1, y, z)$	3.31(1)
O(2B)	C(23A)	3.34(1)
O(2D)	C(31A) $(x, y, z + 1)$	3.34(1)
O(2D)	C(32A) $(x, y, z + 1)$	3.36(2)
O(2D)	C(21C) $(x, y, z + 1)$	3.44(2)
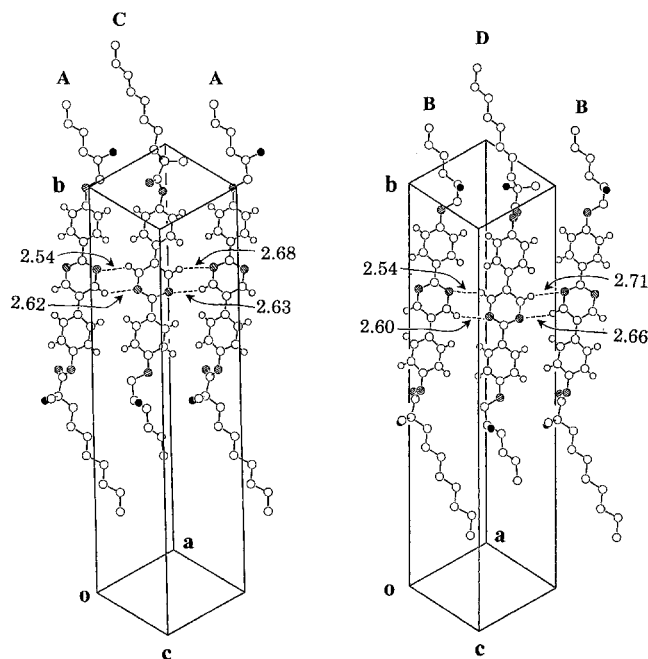
Figure 4. Mutual arrangement of molecules. Atoms are designated as in figure 2. H atoms in chains are omitted for simplicity. F(1) atoms of molecules B and C are almost hidden. Numerical values are interatomic distances of N…H in Å.
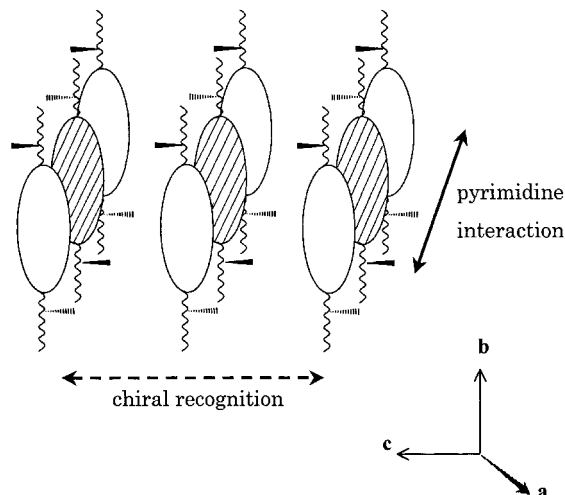
Figure 5. Schematic diagram of crystal packing showing the directions of specific interactions. White and hatched molecules are antiparallel to each other.

figure 5. The chiral recognition seems to stabilize the parallel arrangement of the molecular row, in which the antiparallel packing of molecules is stabilized by the strong interaction between pyrimidine moieties, as mentioned above. Thus, intermolecular interactions within the layer are considered to be heterogeneous: core moieties aggregate rather loosely as a whole, but with locally strong interactions. With respect to the relationship between crystal packing and the IsoX phase, the layer structure with stereo-specific chiral interactions would partially remain due to locally strong interactions at high temperature, leading to the IsoX phase.

4. Conclusions

In the crystal structure of a dichiral mesogen with a unique phase transition to an isotropic mesophase, the aromatic rings have a characteristic packing differ-ing from the usual herringbone arrangement. Strong interactions between pyrimidine rings of antiparallel molecules exist, leading to the large overlapping of core moieties and strong interactions between chiral groups, this being considered to be responsible for the existence of the isotropic mesophase.

References

[1] YOSHIZAWA, A., UMEZAWA, J., ISE, N., SATO, R., SOEDA, Y., KUSUMOTO, T., SATO, K., HIYAMA, T., TAKANISHI, Y., and TAKEZOE, H., 1998, *Jpn. J. appl. Phys.*, **37,** L942.
[2] TAKANISHI, Y., TAKEZOE, H., YOSHIZAWA, A., KUSUMOTO, T., and HIYAMA, T., 2000, *Mol. Cryst. liq. Cryst.*, **347,** 257.
[3] KUSUMOTO, T., SATO, K., KATOH, M., MATSUTANI, A., YOSHIZAWA, A., ISE, N., UMEZAWA, J., TAKANISHI, Y., TAKEZOE, H., and HIYAMA, T., 1999, *Mol. Cryst. liq. Cryst.*, **330,** 227.
[4] YOSHIZAWA, A., ISE, N., KUSUMOTO, T., TAKANISHI, Y., TAKEZOE, H., and HIYAMA, T., *Mol. Cryst. liq. Cryst.* (in the press).
[5] DEBAEDEMAEKER, T., TATE, C., and WOOLFSON, M. M., 1985, *Acta Cryst.*, **A41,** 286.
[6] SHELDRICK, G. M., 1993, SHELXL93. Program for the Refinement of Crystal Structures, University of Göttingen, Germany.
[7] WILSON, A. J. C. (editor), 1992, *International Tables for Crystallography*, Vol. C (Dordrecht: Kluwer Academic Publishers).
[8] WINTER, G., HARTUNG, H., and JASKOLSKI, N., 1987, *Mol. Cryst. liq. Cryst.*, **149,** 17.
[9] WINTER, G., HARTUNG, H., BRANDT, W., and JASKOLSKI, N., 1987, *Mol. Cryst. liq. Cryst.*, **150,** 289.
[10] HORI, K., and TSUJI, C., 1998, *Ferroelectrics*, **212,** 301.
[11] ITO, K., and HORI, K., 1995, *Bull. chem. Soc. Jpn.*, **68,** 3347.
[12] HORI, K., and KAWAHARA, S., 1996, *Liq. Cryst.*, **20,** 311.
[13] GLUSKER, J. P., LEWIS, M., and ROSSI, M., 1994, *Crystal Structure Analysis for Chemists and Biologists* (New York: VCH), p. 647.
[14] BONDI, A., 1964, *J. phys. Chem.*, **68,** 441.